Composite Structures 145 (2016) 80–88

Contents lists available at ScienceDirect

Composite Structures

journal homepage: www.elsevier.com/locate/compstruct

freepaper.me FREE paper

Elasticity alternatives to generalized Vlasov and Timoshenko models for composite beams

Paul R. Heyliger *

Department of Civil and Environmental Engineering, Colorado State University, Fort Collins, CO 80523, United States

ARTICLE INFO

Article history:
Available online 2 March 2016

Keywords:
Beams
Composite
Vlasov
Timoshenko
Ritz

ABSTRACT

The static response of homogeneous and composite beams is studied using approximations of the pointwise displacement components of linear three-dimensional elasticity theory. This method differs from many one-dimensional theories in that the displacements over the beam cross-section are allowed to vary rather than limiting the kinematic model at the start of the analysis. Polynomial approximations are used over the beam cross-section with the resulting integrals computed over the subdomains of differing materials. Several example problems are considered and results are compared with highly accurate one-dimensional beam theories, with very good agreement being found.

© 2016 Elsevier Ltd. All rights reserved.

1. Introduction

The response of composite beams to external forces has seen tremendous recent development that has extended the ability to predict the displacement and stress fields within a wide class of structure. Early studies of beam mechanics focussed primarily on homogeneous materials under what could be described as flexural motion, leading to relatively simple yet powerful theories that are still in common use [1]. These early representations were typically separated from coupling that could occur between flexural response and torsional response, where the latter behavior was characterized not by transverse motion but by an angle of twist about the longer axis of the beam and usually generated by an applied torque about that same axis. Basic beam response changes significantly when the material properties or the beam geometry allow for interaction between bending and twisting types of motion.

Additional changes in beam behavior can be observed when beams are composed of elements that have one dimension of the cross-section that is significantly larger than the other. These elements are common in engineering design and are usually based on optimizing the amount and location of material used to construct the beam section. Early studies of isotropic beams of this nature were presented by Wanger and Pretschner [2], Bleich and Bleich [3], and Kappus [4]. The significant adaptation of a powerful generalized thin-wall theory for beams of open cross-section was given by Vlasov [5], and a number of other important contributions have been summarized in the work of Gjelsvik [6].

In the latter part of the 20th century, a large body of work was developed for thin-walled beams composed of anisotropic and possibly composite materials. The studies of Volovoi and co-workers [7], Yu and co-workers [8–10] and especially Hodges [11] demonstrated the development of robust and highly accurate beam models for the analysis of composite beams. These models are frequently and nobly linked and labeled as extensions to original theories of Vlasov [10] and Timoshenko [8]. They have seen extensive use and are well-known to provide excellent predictions of both the global displacements and the stress fields for both isotropic and composite beams.

One feature of generalized Vlasov and Timoshenko beam models is the necessity to represent the response over the cross-section of the beam, often using two-dimensional finite element approximations, to calculate the effective stiffnesses that characterize global response. In the present work, an approximate model based on the three-dimensional theory of elasticity is used as an alternative to these one-dimensional theories. This type of representation of beam kinematics is not new but has only recently been applied to the study of composite beams. In one sense, elasticity-based models are more complex than one-dimensional models because they use approximations of pointwise displacements everywhere in the beam rather than using general kinematic variables that represent behavior over the beam cross-section. Yet frequently, as in the present case, they can be simpler in application. Because of the nature of the approximations used and the structure of the discretized problem, it could be argued that elasticity-based models are easier to develop and apply. This method is presented here as

* Tel.: +1 970 491 6685 (O); fax: +1 970 491 7727.
E-mail address: prh@engr.colostate.edu

http://dx.doi.org/10.1016/j.compstruct.2016.02.072
0263-8223/© 2016 Elsevier Ltd. All rights reserved.

an alternative to existing one-dimensional theories that can provide reasonable estimates to composite beam response with a relatively low investment of computational effort.

2. Theory

In this section, the general theory behind the elasticity-based model of composite beam deformation is presented along with a detailed account of the types of approximations used to solve the governing equations. Additional details are provided related to practical considerations in applying this methodology.

2.1. Geometry

General three-dimensional solids are considered in which the cross-section coordinates usually identified with one-dimensional beam theories are defined in the (x_1,x_2) or (x,y) plane with a much larger dimension in the x_3 or z axis with a length of L. The beam is assumed to be composed of potentially dissimilar anisotropic materials where the principal material axes are originally aligned with the (x,y,z) axes and then possibly rotated in an arbitrary fashion. For the present study, these materials are assumed to be originally orthotropic and potentially having gone through a rotation in the x–z plane about the y-axis. Hence the original *1*-direction is finally located at an angle θ as measured from the positive z axis. This introduces in-plane shear coupling through the rotated components of the elastic stiffness tensor, with additional coupling between types of deformation being introduced with the presence of dissimilar materials over the beam length or cross-section.

It is further assumed that there is no change in cross-sectional properties along the length of the beam in the z-direction, and that any dissimilar materials are perfectly bonded together at any interface. Under static load, each material is completely defined in terms of the elements of the rotated elastic stiffness tensor, usually expressed in contracted notation as C_{ij}.

2.2. Governing equations

The governing equations used for this study are the three-dimensional equations of linear elasticity with an anisotropic constitutive tensor that can represent what amounts to a monoclinic material. These are not solved explicitly at each point in the domain, but instead approximate solutions are sought for their weak form as expressed within the Principle of Virtual Work. This is usually expressed in indicial form as

$$0 = \int_V \sigma_{ij}\delta\epsilon_{ij}dV - \int_V f_i\delta u_i dV - \int_S t_i\delta u_i dS \tag{1}$$

Here σ_{ij} are the components of Cauchy stress, V is the total volume of the solid, δ is the variational operator, ϵ_{ij} are the components of infinitesimal strain, f_i and t_i are the components of the body force and surface traction vectors, respectively, and S is the total surface of the solid. Expanding the summation gives

$$\begin{aligned} 0 = &\int_V \{\sigma_{xx}\delta\epsilon_{xx} + \sigma_{yy}\delta\epsilon_{yy} + \sigma_{zz}\delta\epsilon_{zz} + \sigma_{yz}\delta\gamma_{yz} + \sigma_{xz}\delta\gamma_{xz} + \sigma_{xy}\delta\gamma_{xy}\}dV \\ &- \int_V (f_x\delta u + f_y\delta v + f_z\delta w)dV \int_S (t_x\delta u + t_y\delta v + t_z\delta w)dS \end{aligned} \tag{2}$$

Here it is understood that the 1, 2, and 3 directions in indicial notation are $(x_1 = x, x_2 = y,$ and $x_3 = z)$, and the engineering shear strains γ_{yz}, γ_{xz}, and γ_{xy} have been introduced where, for example, $\gamma_{yz} = 2\epsilon_{yz}$.

The general constitutive law that links the Cauchy stress to the components of infinitesimal strain ϵ_{ij} can be written as

$$\sigma_{ij} = C_{ijkl}\,\epsilon_{kl} \tag{3}$$

This relationship is commonly expressed in matrix form for the type of materials considered in this study as

$$\begin{Bmatrix} \sigma_{xx} \\ \sigma_{yy} \\ \sigma_{zz} \\ \sigma_{yz} \\ \sigma_{xz} \\ \sigma_{xy} \end{Bmatrix} = \begin{bmatrix} C_{11} & C_{12} & C_{13} & 0 & 0 & C_{16} \\ C_{12} & C_{22} & C_{23} & 0 & 0 & C_{26} \\ C_{13} & C_{23} & C_{33} & 0 & 0 & C_{36} \\ 0 & 0 & 0 & C_{44} & C_{45} & 0 \\ 0 & 0 & 0 & C_{45} & C_{55} & 0 \\ C_{16} & C_{26} & C_{36} & 0 & 0 & C_{66} \end{bmatrix} \begin{Bmatrix} \epsilon_{xx} \\ \epsilon_{yy} \\ \epsilon_{zz} \\ \gamma_{yz} \\ \gamma_{xz} \\ \gamma_{xy} \end{Bmatrix} \tag{4}$$

The stiffness components C_{ij} are associated with either a naturally occurring monoclinic material with 13 independent elastic constants or a rotated orthotropic material. In the latter case, the final C_{ij} as listed in the 6×6 matrix are a function of the on-axis elastic constants and the angle of rotation of originally orthotropic properties about the 3 or z axis. Their explicit forms are given by Reddy [12]. The strain components can be linked with the three displacement components u, v, and w in the x, y, and z directions as

$$\begin{aligned} &\epsilon_{xx} = \frac{\partial u}{\partial x} \quad \epsilon_{yy} = \frac{\partial v}{\partial y} \quad \epsilon_{zz} = \frac{\partial w}{\partial z} \\ &\gamma_{yz} = \frac{\partial v}{\partial z} + \frac{\partial w}{\partial y} \quad \gamma_{xz} = \frac{\partial u}{\partial z} + \frac{\partial w}{\partial x} \quad \gamma_{xy} = \frac{\partial v}{\partial x} + \frac{\partial u}{\partial y}. \end{aligned} \tag{5}$$

These expressions can then be substituted into the statement of virtual work to give an expression that contains the variables u, v, and w along with their variations δu, δv, and δw. For brevity, this expression is not included here.

2.3. The Ritz model

The computational approach used in this study relaxes many of the assumptions used in most beam theories. Rather than introducing specific displacement fields over the beam domain, the three point-wise displacement components are approximated directly using the weak form obtained within virtual work and the Ritz method [13]. There is no need to represent any rotational variables or their equivalent in this theory, since each of the displacements is computed at every location in the beam.

The general form for each of the three displacement approximations can be expressed as

$$u_i(x_j) = \phi_o^{u_i}(x_j) + \sum_{p=1}^{N} A_{ip}\phi_p^{u_i}(x_j) \tag{6}$$

Here the A_{ip} represent constants that are treated as the global unknowns of the problem. The three values of i indicate that there are three components of displacement with $u_1 = u$, and so on. The ϕ_o terms represent the simplest functions that satisfy the essential boundary conditions for that displacement direction. For the cases discussed in this paper, all essential boundary conditions are assumed to be zero. The ϕ_o terms are, therefore, all equal to zero. In the remaining approximations, ϕ_p represent a selected approximate function for each respective direction. These functions must satisfy general requirements of independence as outlined by Reddy [13]. By using a sufficient number of these approximation terms for each displacement component, very accurate solutions can be determined for the displacements.

For each of the three variables u, v, and w that exist at every point over both the beam cross-section and the beam length, polynomial series are used to approximate the beam response. This class of approximation has been used numerous times to represent the deformation of a wide array of solids, particularly early studies in free vibration. Demarest [14] used Legendre polynomials over

freepaper.me FREE paper

the three Cartesian coordinate directions to find the natural modes of vibrating parallelepipeds. This method was extended by Ohno [15], who also discussed the splitting of the resulting eigenvalue problem into a smaller number of equivalent eigenvalue problems using group theory. Polynomial expansions were also used in general cylinder [16] and sphere [17] vibrations. A significant and powerful expansion of this approach was introduced by Visscher [18], who expanded the three displacement components in terms of power series regardless of the shape of the solid. This is generally written for any generic approximation function as

$$\phi_p^u(x,y,z) = x^i y^j z^k \tag{7}$$

This is a very attractive family of approximations in that it frequently yields very simple integration results over the domain of the solid. This type of approximation has seen application in resonating solids [19], vibrating beams [20], and related areas such as granular media [21]. In terms of applications to solids with more general beam geometry, Carrera and co-workers have recently developed a unified beam theory using a modification of this type of approximation over the beam cross section and have extensively applied it to a wide array of problems [22–25]. It has also been used to study the buckling behavior of auxetic and anisotropic beams [26] and the free-vibration behavior of thin-walled beams [27].

If the displacement constants A_{ip} are replaced with the letters c, d, and e for the three displacements (where i takes values associated with the displacements $1 = u, 2 = v, 3 = w$) for any index p, it is possible to generalize the matrix form of the Ritz model. Substitution of the general Ritz approximation into the general weak form leads to a linear system of equations in terms of the unknown constants that can be represented in matrix form as

$$\begin{bmatrix} [K^{11}] & [K^{12}] & [K^{13}] \\ [K^{21}] & [K^{22}] & [K^{23}] \\ [K^{31}] & [K^{23}] & [K^{33}] \end{bmatrix} \begin{Bmatrix} \{c\} \\ \{d\} \\ \{e\} \end{Bmatrix} = \begin{Bmatrix} \{F^u\} \\ \{F^v\} \\ \{F^w\} \end{Bmatrix} \tag{8}$$

The elements of the coefficient matrix ($[K]$) and right-hand side vector$[F]$ are given in Appendix A.

All beams considered in this study are compared with cases in the literature that are under fixed conditions at one end of the beam and are loaded in some fashion at the other end. Hence simple power series are used in all directions (x,y,z) of the bounded solid, although the number and type of the approximation can be adjusted depending on the type of deformation expected for a given loading. For fixed boundary conditions at $z = 0$, all three displacements are equal to zero at every location of the cross-section. More formally, this is expressed as

$$u(x,y,0) = v(x,y,0) = w(x,y,0) = 0 \tag{9}$$

Unlike usual beam theories, the current model does not require the specification of any of the spatial gradients of these displacements as essential boundary conditions. Hence the power-series class in the z-direction can be applied where the exponent in z is equal to or greater than one to satisfy the essential boundary conditions at the fixed support. The approximations in x and y and the evaluation of the element matrices are discussed in the next section.

2.4. Calculations

Computationally, using global power series over the cross-section greatly simplifies the integration required for the relevant coefficient matrices and in fact is one reason why this type of approximation has some appeal. In this study, the cross-sections are limited to solid rectangles, I-beams, and hollow rectangles. Solid sections of regular geometry, including but not limited to rectangles, circles, ellipses, are easily evaluated in closed form. For hollow sections, the integration can be completed first over the outer bounding dimensions of the solid and then subtracting the same integral evaluated over the inner bounding surfaces of the same cross-section. For I-beams, the integration can be completed piecewise by calculating the necessary integrals over each sub-domain of the cross-section. The global derivatives of the power series are likewise power series of lower order that are evaluated in similar fashion. Although the integrals over the beam length are very simple for the case of the cantilevered beams considered in this study, more complex boundary conditions can be handled with minor adjustment [27].

One additional advantage of using global approximation functions over the beam cross-section and length is the potential to group the specific approximations according to the physical character of the displacement components they are being used to represent. This grouping was originally suggested for the case of vibration behavior [15,28], but the same principles can be applied to static deformation. For example, in a bending type of deformation of a symmetric cross-section, terms used to approximate transverse displacement that are odd in the x variable (i.e. the horizontal coordinate of the beam cross-section) can be discarded from the approximation since any displacement of this nature would never be physically realized. Rather than generalizing this discussion for the arbitrary case, these features are discussed for the specific geometries considered in the present study.

3. Numerical results

A number of example geometries and material combinations are considered in this section and the results are compared with existing solutions that have been developed using other highly accurate theories that are known to provide excellent results.

3.1. The thin isotropic strip

First considered is the thin isotropic strip under a twisting moment as studied by Yu and co-workers [10]. The strip is a solid rectangle with width of 0.953 inches and a height of 0.03 inches, with a length of $L = 10$ in. The isotropic strip has $E = 10 \times 10^6$ psi and $v = 0.3$. The loading is applied as two equal and opposite vertical forces of 0.001 lb (in the y-direction) at $(-0.953/2, 0, 10)$ and at $(-0.953/2, 0, 10)$. These forces and their impact are imposed via an equivalent surface traction over the end of the beam where in the absence of body forces the right-hand side forcing function vector takes the form

$$F_i^v = \int_S t_y \Psi_i^v dS = 0.001\Psi_i^v(0.953/2,0,10) - 0.001\Psi_i^v(-0.953/2,0,10) \tag{10}$$

The primary variable of interest is the angle of twist at the end of the strip. Because an elasticity approach is used and twist angle is not treated as a kinematic unknown, the same methodology is used as in a three-dimensional finite element model of Yu and co-workers [10] where the angle is taken to be the vertical displacement at the point of application of load divided by the half-width. Because of material symmetry and the nature of the loading, the centroid of the beam does not move in its cross-sectional plane.

For this problem and those that follow, convergence studies were completed to determine the order of terms necessary for an accurate solution. This procedure is explained in detail for the isotropic strip as an example on similar procedures followed for the other geometries and material combinations. The displacement field with the most complexity is the axial displacement component w. This has both cross-sectional (x,y) dependence as well as axial (z) dependence. In Table 1, the in-plane odd powers are fixed at terms up to and including $x^{11}y^{11}$ and the axial power of z is

freepaper.me FREE paper

Table 1
Convergence of end rotation of isotropic strip: axial terms.

	Highest power along axial direction							
	2	3	4	5	6	7	8	9
$\theta \times 10^2$	22.08	26.09	27.47	28.07	28.37	28.52	28.59	28.60

Table 2
Convergence of end rotation of isotropic strip: axial displacement.

	Combinations of in-plane approximations					
	x^1y^1	x^3y^3	x^5y^5	x^7y^7	x^9y^9	$x^{11}y^{11}$
$\theta \times 10^2$	28.15	28.23	28.36	28.46	28.57	28.60

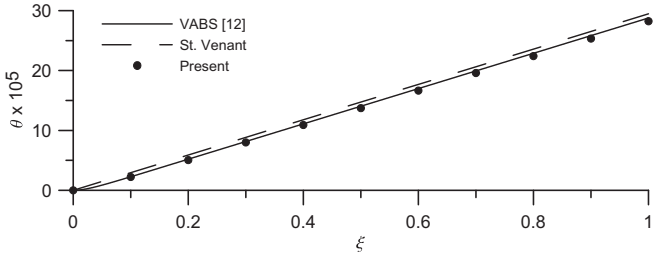

Fig. 1. The angle of twist (in radians) as a function of the dimensionless axial coordinate $\xi = x/L$ for the isotropic strip under an end torque.

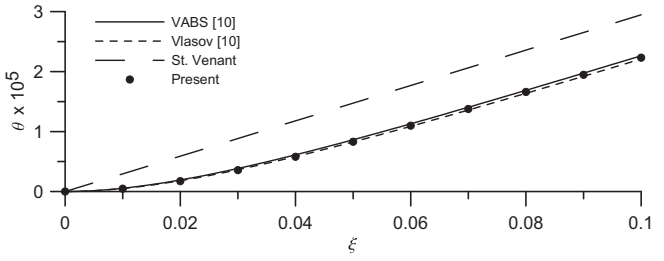

Fig. 2. The rate of change of angle of twist (in radians) as a function of the dimensionless axial coordinate $\xi = x/L$ for the isotropic strip under an end torque.

varied from quadratic to ninth order. Axial polynomial approximations of up to sixth order result in less than one percent difference of terms up to ninth order. For the in-plane variation, with the axial variation fixed at all terms up to and including z^9, approximations are varied from bilinear (x^1y^1) to eleventh order ($x^{11}y^{11}$) as shown in Table 2. Even for relatively low orders of approximation, the accuracy of the model appears to be quite good. For the results in this section, approximations up to and including $x^{11}y^{11}z^9$ were used for w. The in-plane displacements u and v converge at a much lower order, and approximations up to and including $x^3y^3z^9$ were used.

The resulting angle of twist is given in Fig. 1 over the length of the strip and in Fig. 2 for the tenth of the strip length closest to the fixed support. The results are compared with the St. Venant torsion theory, the Vlasov torsion theory, and the VABS model of Yu and co-workers [10]. The latter two are indistinguishable on this plot, and for the most part the results of the present model are in excellent agreement with these two models with a very small underprediction in the angle of twist given by the present models.

Another key variable in several one-dimensional beam theories is the rate of change of the angle of twist. This is typically denoted as θ' in the literature, where the prime superscript is used here to

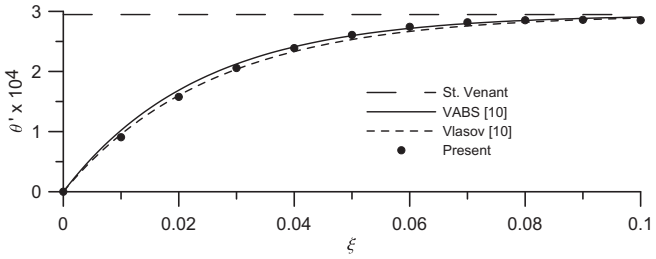

Fig. 3. A closer look at the rate of change of angle of twist (in radians) as a function of the dimensionless axial coordinate $\xi = x/L$ for the isotropic strip under an end torque for the tenth of the strip length closest to the fixed support.

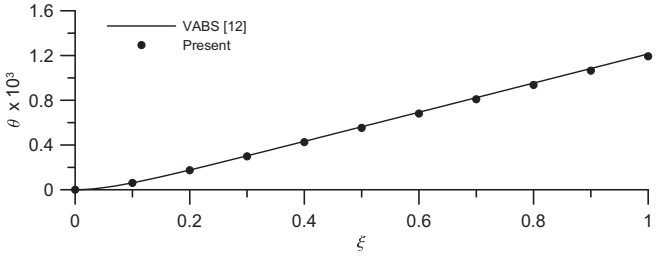

Fig. 4. The angle of twist (in radians) as a function of the dimensionless axial coordinate $\xi = x/L$ for the orthotropic strip under an end torque.

denote the rate of change with respect to the nondimensionalized axial coordinate $\xi = x/L$. For the present model, since the displacement components are approximated using power series in the spatial coordinates, the rate of change of the angle of twist is computed using

$$\theta' = \frac{1}{0.953/2}\frac{\partial v}{\partial z}\frac{dz}{d\xi} \tag{11}$$

The results are shown in Fig. 3, in which an excellent correspondence is observed with the very accurate VABS model of Yu and co-workers [10].

3.2. The orthotropic strip

An increase in complexity over the isotropic strip can be achieved by considering the case of an orthotropic material. Here the elastic constants are those of Yu and co-workers and are taken to be $E_1s = 20.59 \times 10^6$ psi, $E_2 = E_3 = 1.42 \times 10^6$ psi, $G_{12} = G_{13} = 8.70 \times 10^5$ psi, $G_{23} = 6.96 \times 10^5$ psi, and $\nu_{12} = \nu_{13} = \nu_{23} = 0.42$. The *1*-direction implied by the subscripts on elastic modulus are aligned with the *z*-direction. The difference in material response, depending on the loading applied, can be significant for this class of material since the ratio of elastic modulus to shear modulus is no longer related as in the case of the isotropic solid. Instead, these parameters are independent and the ratio is much higher than that of the isotropic case. In the present example, the same loadings are applied as in the isotropic solid, with results for the twist and rate of twist shown in Figs. 4 and 5. Once again, because of material symmetry and the nature of the loading, there is no displacement of the beam centroid, and the rotation and rotation rate are computed using the vertical displacements.

3.3. The anisotropic strip

For the anisotropic case the same strip geometry and loading are used except that the *1*-direction is now oriented at 15° from the *z*-direction. For any angle other than 0° or 90°, there is now

freepaper.me FREE paper

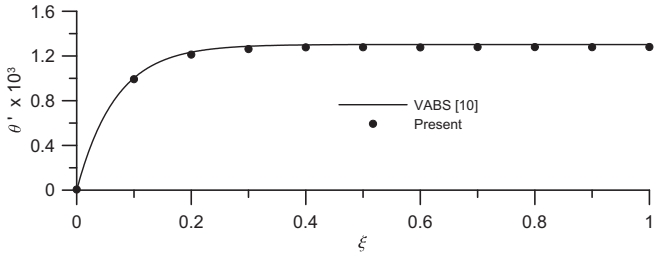

Fig. 5. The rate of change of angle of twist (in radians) as a function of the dimensionless axial coordinate $\xi = x/L$ for the orthotropic strip under an end torque.

coupling between the torsional deformation and bending. For this loading and geometry, the beam centroid moves vertically, and so those displacements must be subtracted before being divided by the half-width of the beam to compute the appropriate slope. The results are shown in Fig. 6 and again show excellent agreement with existing composite beam theory results.

3.4. The isotropic I-beam

A more challenging example of an open cross-section is the I-beam shown in Fig. 7. This beam can be composed of either a homogeneous isotropic material or composed of laminated layers of orthotropic material oriented at varying angle orientations. Both are considered here. In both cases, the material properties were the same as those used for the thin strip.

For the examples considered in this work, the width b was set equal to 1 in. and the height h was taken as 0.5 in. and all wall thicknesses were 0.04 in. The overall length of the beam was taken as 10 in. Once again, a torsional moment was imposed by applying point loads at two locations at the unrestrained end of the beam. In this case, these are applied at the geometric positions of $(0, 0.25, 10)$ and $(0, -0.25, 10)$.

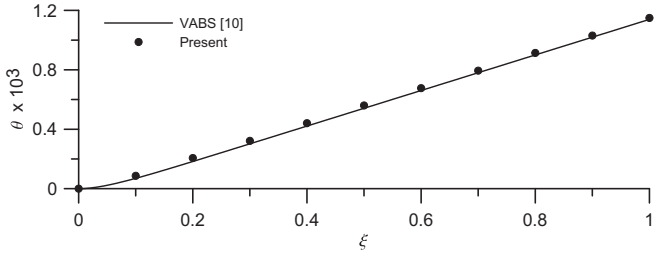

Fig. 6. The angle of twist (in radians) as a function of the dimensionless axial coordinate $\xi = x/L$ for the anisotropic strip under an end torque.

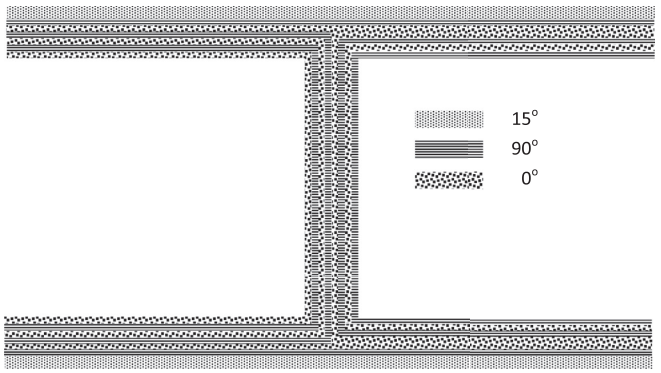

Fig. 7. The lamination scheme of the composite I-beam.

Convergence studies were completed to include a sufficient numbers of terms used to capture the rotation and rotation rate along the beam axis and the values of the axial normal stress. An example of the stress convergence is shown in Table 3, where the in-plane variation of the axial displacement w is shown along with the value of maximum normal stress σ_{zz} in the cross-section for a beam with terms up to seventh order along the z axis. The stress components were computed using the full constitutive law along with the necessary pointwise gradients of the displacement field as computed within the computational model.

Since this section is symmetric, there is no vertical motion of the beam centroid and the rotational angle was taken by measuring the angle created by $u(0, 0.25, 10)$. For the case of the isotropic I-beam, the u and v displacements were computed using only a single odd term in y and x, respectively, along with 7 terms in the axial z direction. The w displacement was computed using odd terms up to order 13 in both x and y for rotation and rotation rate. Hence, there were a total of $(1) * 7 + (1) * 7 + (7 * 7) * 7 = 357$ degrees of freedom used to represent the complete deformation of the beam.

The rotation as a function of dimensionless beam length ξ is shown in Fig. 8, and the rate of change in twist shown in Fig. 9. A contour plot of the axial stress σ_{zz} is given in Fig. 10 and the maximum axial stresses are given in Table 4. Yu and co-workers [10] have generated comparisons with St. Venant, Vlasov, and VABS theories and also a three-dimensional finite element model with 8 elements through the web and flange thickness, 20 elements across each flange, and 10 elements along the web. A total of 100 elements were used along the length, giving a total of 40,000 elements, 46,359 nodes, and 139,077 total degrees of freedom. Comparisons of the maximum axial stress are given in Table 4, with very good agreement between the present model, three-dimensional finite element results, and the VABS model.

3.5. The composite I-beam

A laminated I-beam was also studied using this methodology. The specific geometry has the same dimensions as for the isotropic case but is now divided into anisotropic layers with the stacking sequence as shown in Fig. 7. This geometry has been studied by a number of authors, most prominently because of the initial theoretical and experimental work of Chandra and Chopra [29]. It has also been studied by Volovoi and co-workers [7] and Yu and co-workers [9,10]. The overall width of the beam cross section is 1 in., the total height is 0.5 in. (this corrects a typo in the diagram of Yu and co-workers [9]), and the thickness of both web and flange is 0.04 in. The outer two layers of the flange section are oriented at 15° from the long axis of the beam, and all other layers are oriented at either 0° or 90°. Chandra and Chopra originally gave only the four in-plane elastic constants necessary for the Vlasov beam model used in their theoretical predictions. These are the same in-plane properties as used for the orthotropic strip of the present work except $G_{12} = 8.9 \times 10^5$ psi. Two different length configurations are considered with slight adjustments in the elastic constants used for each case. These are described separately below.

Table 3
Convergence of maximum stress (psi) for isotropic I-beam: axial displacement.

Powers of z	Powers of x			
	x^5	x^7	x^9	x^{11}
z^5	166.9	221.6	277.4	317.4
z^7	334.5	368.0	388.9	404.3
z^9	334.9	378.1	409.5	433.8
z^{11}	402.2	420.5	432.8	–

freepaper.me FREE paper دانلود کننده مقالات علمی

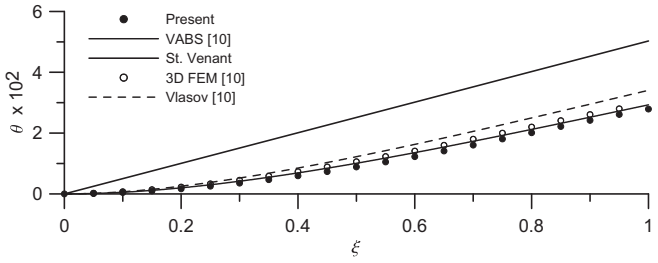

Fig. 8. The angle of twist (in radians) as a function of the dimensionless axial coordinate $\xi = x/L$ for the isotropic I-beam under an end torque.

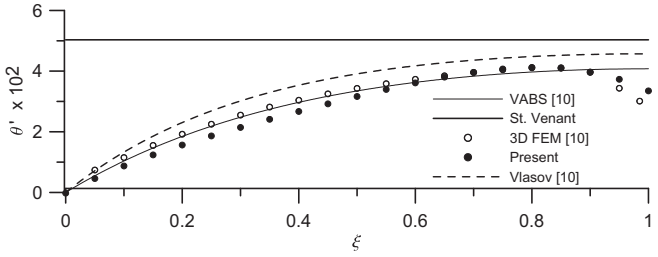

Fig. 9. The rate of change of the angle of twist (in radians) as a function of the dimensionless axial coordinate $\xi = x/L$ for the isotropic I-beam under an end torque.

3.5.1. The shorter I-beam

Yu and co-workers [10] used the exact same properties given for the orthotropic strip in the present work along with a length of 10 in. An applied torque was imposed by applying equal and opposite loads in the same fashion as was used for the isotropic I-beam. The angle of twist was computed by taking the inverse tangent of the angle computed by the horizontal displacement in the cross-section divided by half of the beam height. The end rotation is shown as a function of dimensionless beam length in Fig. 11, where it is compared against the VABS and three-dimensional finite element results of Yu and co-workers [10]. The agreement between the three models is excellent. The rate of change in twist, which to reiterate is not a kinematic variable of the present theory but is used as such in several one-dimensional beam models, is shown in Fig. 12, with the same comparisons as for the end twist. The agreement is reasonably good with the results of the present method being slightly larger than those computed by the three-dimensional finite element model near the loaded end of the beam. The maximum axial stresses are given in Table 4 and are between those of the finite element and VABS results of Yu and co-workers [10].

3.5.2. The longer I-beam

The original composite I-beam geometry of Chandra and Chopra [29] used a beam length of 30 inches and applied two different loadings: a unit end torque and a unit vertical load. For the unit torque, they computed the end twist and compared their results using the Vlasov composite beam theory. Their results are shown in Fig. 13 along with those of the present model. Their Vlasov theory predictions underpredicted the end rotations in a manner that increased as the loaded end was approached. Unfortunately, the measured twist at the loaded end was not given. The present model gives an end twist that is significantly larger than that of the Vlasov theory and also tracks quite well with the experimental results.

The end point loading in the present model was applied at a single location at the centroid of the beam cross-section at the end of the beam length. As in the case of an applied end torque, this is applied in the present model by considering the integrated traction term at the loaded end. The resulting angle of twist and the end slope are both shown in Fig. 14 and are compared with the Vlasov theory and experimental results of Chandra and Chopra [29]. The present results overpredict both experimental and theoretical results but are still in reasonably good agreement.

3.6. Closed sections

One final configuration that can be considered by the present method is the closed rectangular section, which has a mode of deformation significantly different than that for open sections. As noted by Yu and co-workers [9,10], the original Vlasov theory was developed to model thin-walled beams with open cross-sections. The fact that fixed walls add rotational restraint was addressed by the deformation field assumed in such a theory. Yu

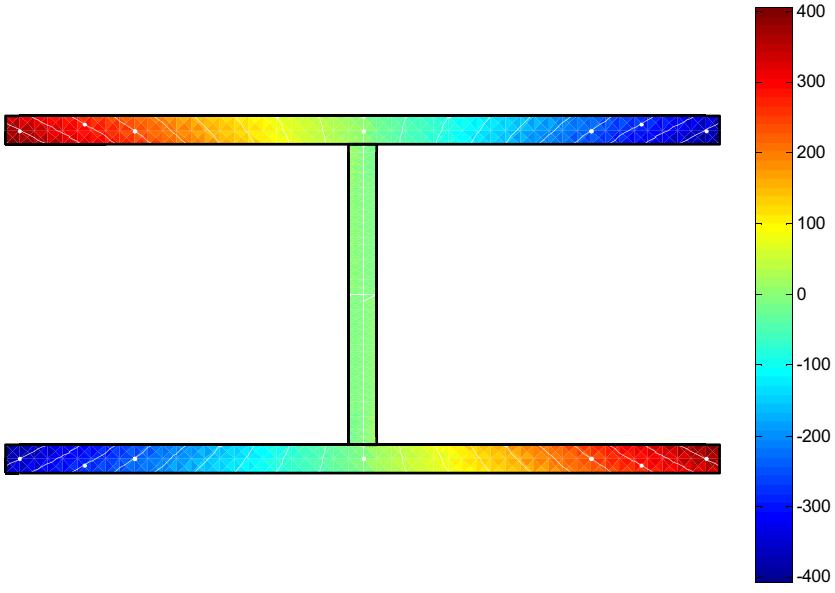

Fig. 10. Axial (normal) stress contours of the isotropic I-beam under constant end torque.

freepaper.me FREE paper

Table 4
Max and min stresses (psi) for the isotropic I-beam.

Material	Variable	Present	FEM [10]	VABS [10]
Isotropic	σ_{zz}^{max}	433.8	430.2	405.6
	σ_{zz}^{min}	−433.8	−430.2	−434.2
Composite	σ_{zz}^{max}	2069	2251	1756
	σ_{zz}^{min}	−2069	−2251	−2052

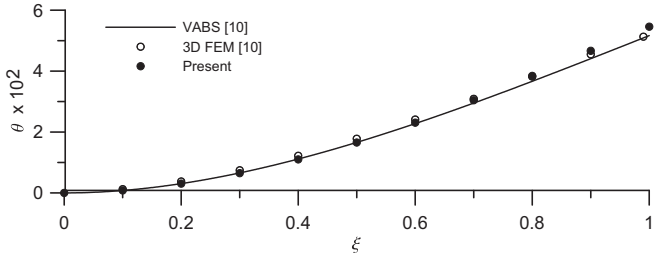

Fig. 11. The angle of twist (in radians) as a function of the dimensionless axial coordinate $\xi = x/L$ for the composite I-beam under an end torque.

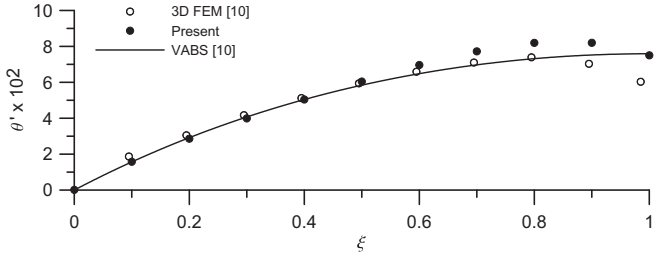

Fig. 12. The rate of change of the angle of twist (in radians) as a function of the dimensionless axial coordinate $\xi = x/L$ for the composite I-beam under an end torque.

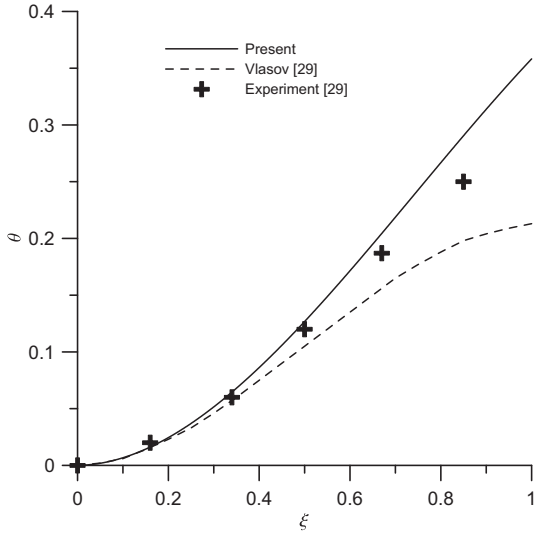

Fig. 13. The angle of twist (in radians) as a function of the dimensionless axial coordinate $\xi = x/L$ for the composite I-beam under an end torque.

and co-workers considered a hollow isotropic rectangle with outer dimensions of 0.953 in. in width, 0.53 in. in height, a constant thickness of 0.03 in. with the isotropic properties used here to model the isotropic strip [10], and an applied end torque induced by equal and opposite vertical loads along the lines of horizontal

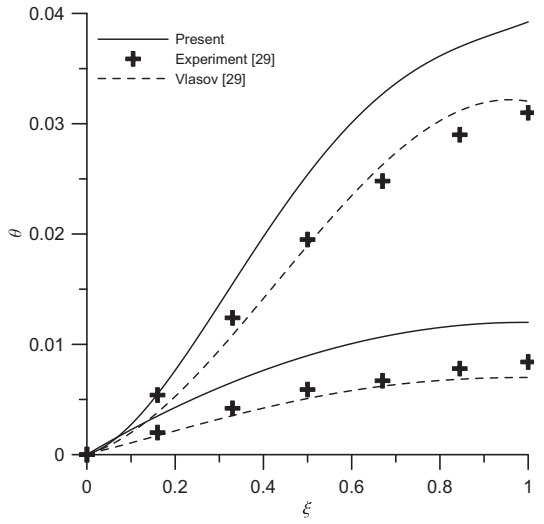

Fig. 14. The angle of twist (in radians, upper range) and end slope (in radians, lower range) as a function of the dimensionless axial coordinate $\xi = x/L$ for the composite I-beam under an end load.

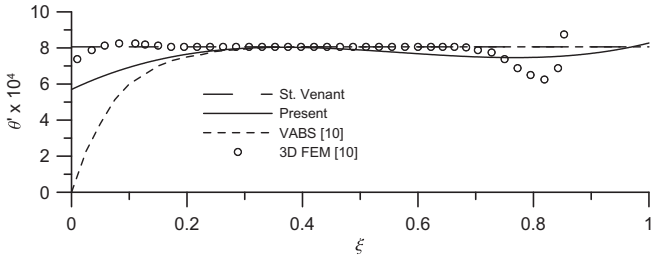

Fig. 15. The rate of change of angle of twist (in radians) as a function of the dimensionless axial coordinate $\xi = x/L$ for the hollow isotropic box beam under an end torque.

symmetry. This geometry admits a St. Venant solution assuming constant shear stresses over the thickness, and has also been solved using three-dimensional finite elements and the VABS generalized Vlasov theory of Yu and co-workers [10]. The results for the rate of change of angle of twist are shown in Fig. 15 as computed using in-plane terms up to 5th order for the axial displacement and in-plane terms up to cubic order for the in-plane displacements, with polynomials up to order four in the axial direction. Yu and co-workers have noted that the VABS generalized theory should not be used for closed-section beams, and instead the VABS classical or generalized Timoshenko models should be used [10]. Use of the present method is not based on any such considerations. The displacement field is described only in terms of the approximation functions used rather than the effects of torsional restraint with good agreement with three-dimensional finite element results. Hence, this class of elasticity model can be used for either closed or open sections.

3.7. Discussion

The use of three-dimensional elasticity approximations to compute the displacement and stress fields gives reasonable results that reflect common trade-offs that must be considered when selecting any beam theory. Advantages of the present approach over either full three-dimensional elasticity finite element models or more complex one-dimensional beam theories include a relatively small number of degrees of freedom required to represent the complete beam, ease of computation and the relative simplicity

freepaper.me FREE paper

Table 5
Summary of end rotations $\theta \times 10^2$ (radians) as a function of dimensionless length ξ.

ξ	Anisotropic strip	Isotropic I-beam	Composite I-beam
0.0	0	0	0
0.1	.6947	.0447	.0823
0.2	.1829	.1677	.3058
0.3	.3018	.3537	.6490
0.4	.4214	.5946	1.101
0.5	.5410	.8865	1.656
0.6	.6607	1.226	2.307
0.7	.7803	1.605	3.043
0.8	.9000	2.011	3.842
0.9	1.020	2.419	4.666
1.0	1.139	2.790	5.458

of the formulation, the potential use of group theory to optimize the selection of the approximation functions, and accuracy. Agreement with other models ranges from excellent for the cases of the isotropic, orthotropic, and anisotropic strips, the isotropic I-beam, and the isotropic hollow rectangle, to more variable agreement for the anisotropic I-beam. To aid in any future comparisons, a summary of end rotations as a function of dimensionless length for three of the beams considered in this study are given in Table 5.

One disadvantage of the present methodology is related to the nature of the approximation functions used for beams that contain any interface between dissimilar layers. The conditions at these locations are such that the displacements and tractions across the interface are continuous. The global polynomials used in the present method meet the first condition, but fail to satisfy the second condition because of the changes in the material properties across the dissimilar material interface. The nature of this change in properties is such that it forces the normal gradient of the primary displacements to be dissimilar on either side of the interface. Both general finite element approximations and the discretization procedure used in many one-dimensional models (such as the VABS theory used for comparison in this study or other beam theories) meet this requirement, whereas the simple power series do not. This difference may be the source of some of the discrepancies between the results considered here.

Improvements short of discretizing the cross-section are possible but were not explored in this work. Polynomial bases with C^0 continuity across dissimilar material interface regions would potentially lead to an increase in accuracy in both the displacement variables and the resulting stresses. Using power series basis functions can also result in global coefficient matrices that are less well-conditioned than other families of approximation. For the results of this study, the order of terms used in the approximation was low enough that this did not appear to be an issue.

Another source of potential discrepancy with existing solutions is in the nature of the axial approximation of the beam. Simple power series in z are used for the present model, but piecewise linear approximations are used in the three-dimensional finite element models compared with here along with an exact one-dimensional solution [10]. The polynomial approximations of the present model could of course be adjusted so that the axial variation either includes different terms than those used here or are also piecewise in the axial direction. The same types of adjustment may be useful in nonlinear deformations, where there may be regions of the beam that may require a more localized representation. As it stands, the present approach would still be quite useful even when the deformations are relatively large, since the updated displacement gradient quantities frequently used in nonlinear analysis can be computed for any load step at any location within the beam.

4. Conclusions

Polynomial series approximations were used to represent pointwise displacements for thin strips, I-beams, and closed thin-walled sections under end point loads and point moments. The following conclusions can be drawn from the results of these analyses:

1. The present model gives rotation and rotation rates that are in excellent agreement with VABS and three-dimensional finite element results for isotropic, orthotropic, and anisotropic thin strips under an end moment.
2. The present model gives rotation, rotation rates, and axial stresses that are in excellent agreement with VABS and three-dimensional finite element for isotropic I-beams under an end moment. For composite I-beams, the present model slightly overpredicts the displacement components.
3. The end twist for the composite I-beam under an end moment are in very good agreement with experiment. For the case of an applied end load, the present model overpredicts the end twist and end rotation when compared to the Vlasov beam theory.
4. For the closed isotropic hollow rectangle cross-section under an end moment, the present model gives a rate of twist behavior that is in reasonably good agreement with three-dimensional finite element results with little change in essential theory or calculation strategy.

Although this method may lack the accuracy necessary to directly compete with more robust beam theories, it offers a reasonable alternative in predicting global response with a moderate amount of computational effort. Other potential benefits await exploration.

Acknowledgements

Support from a Grant from the Mountains Plains Consortium is gratefully acknowledged. Professor Wenbin Yu kindly provided original data for many of the plots.

Appendix A

The elements of the matrix equations for the Ritz model are given as:

$$K_{ij}^{11} = \int_V \left[C_{11}\frac{\partial \Psi_i^u}{\partial x}\frac{\partial \Psi_j^u}{\partial x} + C_{16}\frac{\partial \Psi_i^u}{\partial x}\frac{\partial \Psi_j^u}{\partial y} + C_{55}\frac{\partial \Psi_i^u}{\partial z}\frac{\partial \Psi_j^u}{\partial z} + C_{16}\frac{\partial \Psi_i^u}{\partial y}\frac{\partial \Psi_j^u}{\partial x} + C_{66}\frac{\partial \Psi_i^u}{\partial y}\frac{\partial \Psi_j^u}{\partial y}\right] dV \tag{12}$$

$$K_{ij}^{12} = \int_V \left[C_{12}\frac{\partial \Psi_i^u}{\partial x}\frac{\partial \Psi_j^v}{\partial y} + C_{16}\frac{\partial \Psi_i^u}{\partial x}\frac{\partial \Psi_j^v}{\partial x} + C_{45}\frac{\partial \Psi_i^u}{\partial z}\frac{\partial \Psi_j^v}{\partial z} + C_{26}\frac{\partial \Psi_i^u}{\partial y}\frac{\partial \Psi_j^v}{\partial y} + C_{66}\frac{\partial \Psi_i^u}{\partial y}\frac{\partial \Psi_j^v}{\partial x}\right] dV \tag{13}$$

freepaper.me FREE paper

$$K_{ij}^{13} = \int_V \left[C_{13} \frac{\partial \Psi_i^u}{\partial x} \frac{\partial \Psi_j^w}{\partial z} + C_{45} \frac{\partial \Psi_i^u}{\partial z} \frac{\partial \Psi_j^w}{\partial y} + C_{55} \frac{\partial \Psi_i^u}{\partial z} \frac{\partial \Psi_j^w}{\partial x} + C_{36} \frac{\partial \Psi_i^u}{\partial y} \frac{\partial \Psi_j^w}{\partial z} \right] dV \tag{14}$$

$$K_{ij}^{22} = \int_V \left[C_{22} \frac{\partial \Psi_i^v}{\partial y} \frac{\partial \Psi_j^v}{\partial y} + C_{26} \frac{\partial \Psi_i^v}{\partial y} \frac{\partial \Psi_j^v}{\partial x} + C_{44} \frac{\partial \Psi_i^v}{\partial z} \frac{\partial \Psi_j^v}{\partial z} + C_{26} \frac{\partial \Psi_i^v}{\partial x} \frac{\partial \Psi_j^v}{\partial y} + C_{66} \frac{\partial \Psi_i^v}{\partial x} \frac{\partial \Psi_j^v}{\partial x} \right] dV \tag{15}$$

$$K_{ij}^{23} = \int_V \left[C_{23} \frac{\partial \Psi_i^v}{\partial y} \frac{\partial \Psi_j^w}{\partial z} + C_{44} \frac{\partial \Psi_i^v}{\partial z} \frac{\partial \Psi_j^w}{\partial y} + C_{45} \frac{\partial \Psi_i^v}{\partial z} \frac{\partial \Psi_j^w}{\partial x} + C_{36} \frac{\partial \Psi_i^v}{\partial x} \frac{\partial \Psi_j^w}{\partial z} \right] dV \tag{16}$$

$$K_{ij}^{33} = \int_V \left[C_{33} \frac{\partial \Psi_i^w}{\partial z} \frac{\partial \Psi_j^w}{\partial z} + C_{44} \frac{\partial \Psi_i^w}{\partial y} \frac{\partial \Psi_j^w}{\partial y} + C_{45} \frac{\partial \Psi_i^w}{\partial y} \frac{\partial \Psi_j^w}{\partial x} + C_{45} \frac{\partial \Psi_i^w}{\partial x} \frac{\partial \Psi_j^w}{\partial y} + C_{55} \frac{\partial \Psi_i^w}{\partial x} \frac{\partial \Psi_j^w}{\partial x} \right] dV \tag{17}$$

$$F_i^u = \int_V f_x \Psi_i^u dV + \int_S t_x \Psi_i^u dS \tag{18}$$

$$F_i^v = \int_V f_y \Psi_i^v dV + \int_S t_y \Psi_i^v dS \tag{19}$$

$$F_i^w = \int_V f_z \Psi_i^w dV + \int_S t_z \Psi_i^w dS \tag{20}$$

References

[1] Timoshenko SP. History of strength of materials. New York: Dover; 1983.
[2] Wagner H, Pretschner W. Verdrehung und Knickung von offenen Profilen. Luftfahrtforschung 1934;11:174–80.
[3] Bleich F, Bleich H. Bending, torsion, and buckling of bars composed of thin walls. In: Prelim. pub. 2nd congress of international association for bridge and structural engineers, english ed.; 1936. p. 871.
[4] Kappus R. Twisting failure of centrally loaded open-section columns in the elastic range. Luftfahrtforschung 1937;14:444–57. Translated by Vanier J. National advisory committee for aeronautics, no. 851; 1938.
[5] Vlasov V. Thin-walled elastic beams. 2nd ed. Jerusalem: Israel Program for Scientific Translations; 1963.
[6] Gjelsvik A. The theory of thin-walled bars. New York: John Wiley and Sons; 1981.
[7] Volovoi VV, Hodges DH, Berdichevsky VL, Sutyrin VG. Asymptotic theory for static behavior of elastic anisotropic I-beams. Int J Solids Struct 1999;36:1017–43.
[8] Yu W, Hodges DH, Volovoi VV, Cesnik CES. On Timoshenko-like modeling of initially curved and twisted composite beams. Int J Solids Struct 2002;39:5101–21.
[9] Yu W, Volovoi VV, Hodges DH, Hong X. Validation of the variational asymptotic beam sectional (VABS) analysis. AIAA J 2002;40:2105–12.
[10] Yu W, Hodges DH, Volovoi VV, Fuchs ED. A generalized Vlasov theory for composite beams. Thin Walled Struct 2005;43:1493–511.
[11] Hodges DH. Nonlinear composite beam theory. United States: AIAA; 2006.
[12] Reddy JN. Mechanics of laminated composite plates and shells: theory and analysis. Boca Raton: CRC Press; 2004.
[13] Reddy JN. Energy principles and variational methods in mechanics. New York: Wiley; 2002.
[14] Demarest HH. Cube resonance method to determine elastic constants of solids. J Acoust Soc Am 1971;49:768–75.
[15] Ohno I. Free vibration of a rectangular parallelepiped crystal and its application to determination of elastic constants of orthorhombic crystals. J Phys Earth 1976;24:355–79.
[16] Heyliger PR. Axisymmetric free vibrations of finite anisotropic cylinders. J Sound Vib 1991;148:507–20.
[17] Heyliger PR, Jilani A. The free vibrations of inhomogeneous cylinders and spheres. Int J Solids Struct 1992;29:2689–708.
[18] Visscher WM, Migliori A, Bell TM, Reinert RA. On normal modes of free vibration of inhomogeneous and anisotropic elastic objects. J Acoust Soc Am 1991;90:2154–62.
[19] Migliori A, Sarrao JL. Resonant ultrasound spectroscopy. New York: Wiley; 1997.
[20] Heyliger P, Ugander P, Ledbetter H. Anisotropic elastic constants: measurement by impact resonance. ASCE J Mater Civil Eng 2001;13:356–63.
[21] Heyliger PR. Ritz finite elements for curvilinear particles. Commun Numer Methods Eng 2005;22:335–45.
[22] Carrera E, Petrolo M, Nali P. Unified formulation applied to free vibrations finite element analysis of beams with arbitrary cross-section. Shock Vib 2010;18:485–502.
[23] Carrera E, Giunta G, Petrolo M. Beam structures: classical and advanced theories. New York: John Wiley and Sons; 2011.
[24] Catapano A, Giunta G, Belouettar S, Carrera E. Static analysis of laminated beams via a unified formulation. Compos Struct 2011;94:75–83.
[25] Giunta G, Biscani F, Belouettar S, Carrera E. Analysis of thin-walled beams via a one-dimensional unified formulation through a Navier- type solution. Int J Appl Mech 2011;3:407–34.
[26] Heyliger PR. Continuum-based stability of anisotropic and auxetic beams. Mech Res Commun 2015;69:114–20.
[27] Heyliger PR. Elasticity-based free vibration of anisotropic thin-walled beams. Thin-Walled Struct 2015;95:73–87.
[28] Mochizuki E. Application of group theory to free oscillations of an anisotropic rectangular parallelepiped. J Phys Earth 1987;35:159–70.
[29] Chandra R, Chopra I. Experimental and theoretical analysis of composite I-beams with elastic coupling. AIAA J 1991;29:2197–206.

freepaper.me FREE paper